

This is a repository copy of *Presynaptic accumulation of  $\alpha$ -synuclein causes synaptopathy and progressive neurodegeneration in Drosophila*.

White Rose Research Online URL for this paper:  
<https://eprints.whiterose.ac.uk/174452/>

Version: Published Version

---

**Article:**

Bridi, Jessika C., Bereczki, Erika, Smith, Saffron K et al. (6 more authors) (2021)  
Presynaptic accumulation of  $\alpha$ -synuclein causes synaptopathy and progressive neurodegeneration in Drosophila. *Brain Communications*. fcab049. ISSN 2632-1297

<https://doi.org/10.1093/braincomms/fcab049>

---

**Reuse**

This article is distributed under the terms of the Creative Commons Attribution (CC BY) licence. This licence allows you to distribute, remix, tweak, and build upon the work, even commercially, as long as you credit the authors for the original work. More information and the full terms of the licence here:  
<https://creativecommons.org/licenses/>

**Takedown**

If you consider content in White Rose Research Online to be in breach of UK law, please notify us by emailing [eprints@whiterose.ac.uk](mailto:eprints@whiterose.ac.uk) including the URL of the record and the reason for the withdrawal request.

# BRAIN COMMUNICATIONS

## Presynaptic accumulation of $\alpha$ -synuclein causes synaptopathy and progressive neurodegeneration in *Drosophila*

 Jessika C. Bridi,<sup>1\*</sup>  Erika Berezcki,<sup>2</sup>  Saffron K. Smith,<sup>3</sup> Gonçalo M. Poças,<sup>4,5</sup>  Benjamin Kottler,<sup>1</sup> Pedro M. Domingos,<sup>4</sup> Christopher J. Elliott,<sup>3</sup> Dag Aarsland<sup>6,7</sup> and  Frank Hirth<sup>1</sup>

\* Present address: Laboratory of Molecular and Functional Neurobiology, Department of Pharmacology, Institute of Biomedical Sciences, University of São Paulo, São Paulo 05508-000, Brazil.

Alpha-synuclein ( $\alpha$ -syn) mislocalization and accumulation in intracellular inclusions is the major pathological hallmark of degenerative synucleinopathies, including Parkinson's disease, Parkinson's disease with dementia and dementia with Lewy bodies. Typical symptoms are behavioural abnormalities including motor deficits that mark disease progression, while non-motor symptoms and synaptic deficits are already apparent during the early stages of disease. Synucleinopathies have therefore been considered synaptopathies that exhibit synaptic dysfunction prior to neurodegeneration. However, the mechanisms and events underlying synaptopathy are largely unknown. Here we investigated the cascade of pathological events underlying  $\alpha$ -syn accumulation and toxicity in a *Drosophila* model of synucleinopathy by employing a combination of histological, biochemical, behavioural and electrophysiological assays. Our findings demonstrate that targeted expression of human  $\alpha$ -syn leads to its accumulation in presynaptic terminals that caused downregulation of synaptic proteins, cysteine string protein, synapsin, and syntaxin 1A, and a reduction in the number of Bruchpilot puncta, the core component of the presynaptic active zone essential for its structural integrity and function. These  $\alpha$ -syn-mediated presynaptic alterations resulted in impaired neuronal function, which triggered behavioural deficits in ageing *Drosophila* that occurred prior to progressive degeneration of dopaminergic neurons. Comparable alterations in presynaptic active zone protein were found in patient brain samples of dementia with Lewy bodies. Together, these findings demonstrate that presynaptic accumulation of  $\alpha$ -syn impairs the active zone and neuronal function, which together cause synaptopathy that results in behavioural deficits and the progressive loss of dopaminergic neurons. This sequence of events resembles the cytological and behavioural phenotypes that characterise the onset and progression of synucleinopathies, suggesting that  $\alpha$ -syn-mediated synaptopathy is an initiating cause of age-related neurodegeneration.

- 1 Department of Basic & Clinical Neuroscience, King's College London, Institute of Psychiatry, Psychology & Neuroscience, Maurice Wohl Clinical Neuroscience Institute, London SE5 9RX, UK
- 2 Department of Neurobiology, Care Sciences and Society, Center for Alzheimer Research, Division of Neurogeriatrics, Karolinska Institutet, Novum, Stockholm 171 77, Sweden
- 3 Department of Biology and York Biomedical Research Institute, University of York, York YO1 5DD, UK
- 4 Instituto de Tecnologia Química e Biológica António Xavier, Universidade Nova de Lisboa (ITQB NOVA), Oeiras, Lisbon 2780-157, Portugal
- 5 School of Biological Sciences, Monash University, Melbourne, VIC 34QP+JV, Australia
- 6 Department of Old Age Psychiatry, Institute of Psychiatry Psychology and Neuroscience, King's College London, London, UK
- 7 Centre for Age-Related Diseases, Stavanger University Hospital, Stavanger 4068, Norway

Received October 7, 2020. Revised February 13, 2021. Accepted February 15, 2021. Advance Access publication March 22, 2021

© The Author(s) (2021). Published by Oxford University Press on behalf of the Guarantors of Brain.

This is an Open Access article distributed under the terms of the Creative Commons Attribution License (<http://creativecommons.org/licenses/by/4.0/>), which permits unrestricted reuse, distribution, and reproduction in any medium, provided the original work is properly cited.

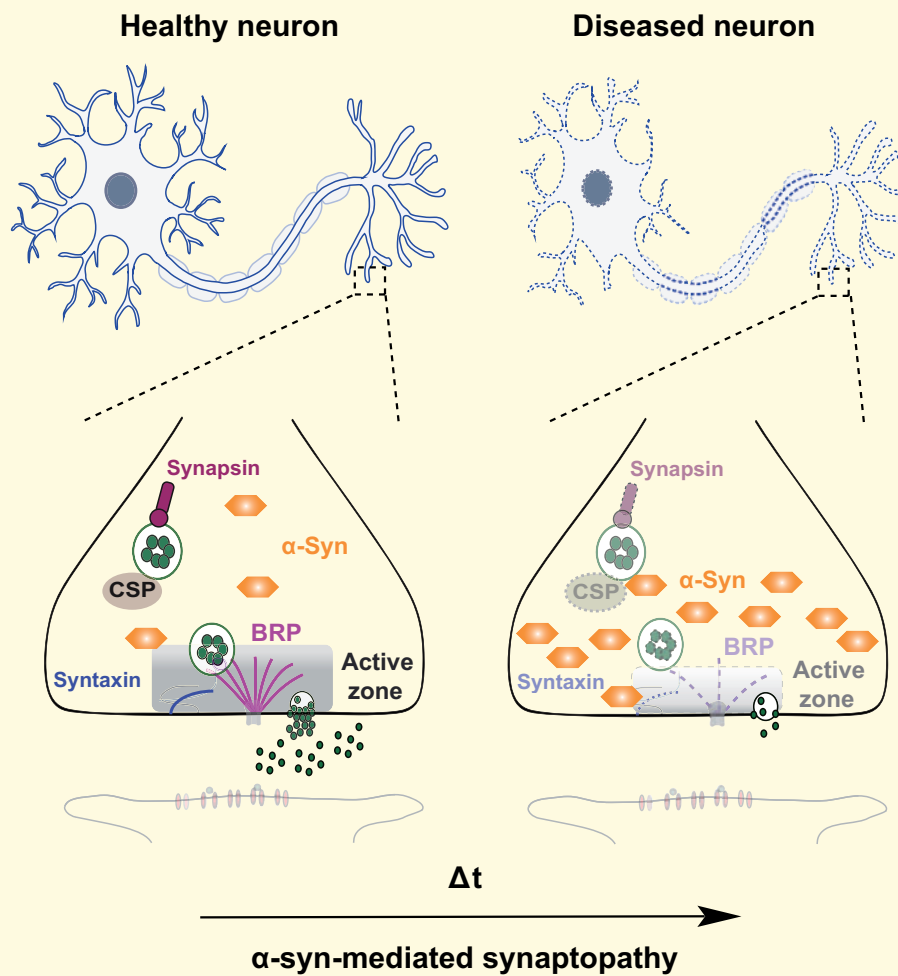
Correspondence to: Frank Hirth  
 Department of Basic & Clinical Neuroscience  
 King's College London, Institute of Psychiatry  
 Psychology & Neuroscience  
 Maurice Wohl Clinical Neuroscience Institute, London, UK  
 E-mail: Frank.Hirth@kcl.ac.uk

Correspondence may also be addressed to: Jessika C. Bridi,  
 E-mails: Jessikabridi@usp.br; jessikacbridi@gmail.com

**Keywords:** Parkinson's disease;  $\alpha$ -synuclein; active zone; synaptopathy; neurodegeneration

**Abbreviations:** AZ = active zone; CSP = cysteine string protein; DA = dopaminergic; DART = *Drosophila* Arousal Tracking system; DLB = dementia with Lewy bodies; iSIM = instant structured illumination microscopy; NMJ = neuromuscular junction; PDD = Parkinson's disease dementia; PER = proboscis extension response; SING = startled-induced negative geotaxis;  $\alpha$ -syn =  $\alpha$ -synuclein.

### Graphical Abstract



Abbrev.: CSP, cysteine string protein; BRP, Bruchpilot

## Introduction

Synucleinopathies are characterized by intraneuronal inclusions called Lewy bodies (LB) that are mainly formed of misfolded and aggregated forms of the pre-synaptic protein  $\alpha$ -synuclein ( $\alpha$ -syn).<sup>1-4</sup> These include

dementia with LB (DLB) as well as Parkinson's disease with dementia (PDD) and Parkinson's disease. Parkinson's disease is mainly characterized by the progressive loss of dopaminergic (DA) neurons in the substantia nigra pars compacta (SN), thereby depleting dopamine levels in synaptic terminals of the dorsal

striatum.<sup>5–7</sup> The resulting regulatory imbalance in the basal ganglia causes a range of behavioural symptoms including bradykinesia, uncontrollable tremor at rest, postural impairment and rigidity.<sup>8–10</sup>

Although the majority of Parkinson's disease cases are sporadic, several genes including *LRRK2*, *Parkin*, *PINK1*, *DJ-1*, *GBA* and *SNCA* contribute to heritable cases of the disease.<sup>11,12</sup> However, among Parkinson's disease-related genes identified, the *SNCA* gene encoding  $\alpha$ -syn remains the most potent culprit underlying Parkinson's disease, with a key pathogenic role both in familial and sporadic cases.<sup>13,14</sup> Several point mutations in *SNCA* and increased gene dosage caused by duplication or triplication of the gene locus, are causally related to severe forms of Parkinson's disease.<sup>15,16</sup> These findings suggest a causal relationship between  $\alpha$ -syn levels and the severity of cognitive decline, motor and non-motor symptoms, and neurodegeneration.<sup>5,17</sup>

Although the mechanisms underlying  $\alpha$ -syn toxicity remain unclear, proteinaceous inclusions enriched with  $\alpha$ -syn were found not only in LB within the neuronal soma but also in axonal processes.<sup>18</sup> Most importantly,  $\alpha$ -syn micro-aggregates were found to be enriched in the presynaptic terminals of DLB patients<sup>19</sup> along with phosphorylated  $\alpha$ -syn, which is believed to disrupt synaptic structure and function.<sup>20</sup> These findings suggest that  $\alpha$ -syn accumulation may cause a toxic gain of function phenotype at the synapse, which impairs its function and connectivity, ultimately causing synaptopathy.

In line with this hypothesis, classical motor symptoms in Parkinson's disease become clinically apparent only when 60% of DA striatal terminals were already lost, while the loss of DA neurons in the SN is only ~30%.<sup>21</sup> Corroborating these observation, it is well acknowledged that the onset of Parkinson's disease initiates at least 20 years prior to the detection of classical motor phenotypes, a period known as the prodromal phase.<sup>16,22,23</sup> It has been suggested that during this phase, a large number of proteins involved in synaptic transmission are affected, as indicated by their altered expression levels in Parkinson's disease and DLB patients.<sup>24,25</sup> These findings are in agreement with positron emission tomography of early-stage Parkinson's disease patients who presented extensive axonal damage and diminished nigrostriatal pathway connectivity.<sup>26</sup> Therefore, it has been hypothesized that neurodegeneration in Parkinson's disease and DLB follows a dying back-like pathomechanism, where degeneration of synapses and axonal connections precedes the loss of neurons, classifying them as synaptopathies.<sup>5,27</sup> However, it remains unclear how  $\alpha$ -syn accumulation impairs synaptic homeostasis, its structure and function, ultimately leading to neurodegeneration.

Here we investigated the succession of events caused by cell and tissue-specific accumulation of  $\alpha$ -syn. We employed a *Drosophila* model of synucleinopathy that expresses human wild-type  $\alpha$ -syn, and analysed post-mortem tissue of Parkinson's disease and DLB patients.

Our findings demonstrate that  $\alpha$ -syn accumulates in, and alters the presynaptic terminal, especially the active zone (AZ), which was also observed in the prefrontal cortex of DLB patients. In *Drosophila*, these alterations caused neuronal dysfunction and behavioural deficits that preceded degenerative loss of DA neurons—cytological and behavioural phenotypes that resemble the onset and progression of synucleinopathies. Together these findings provide experimental evidence that presynaptic accumulation of  $\alpha$ -syn causes synaptopathy and progressive neurodegeneration.

## Materials and methods

### Fly stocks and husbandry

All fly stocks were maintained in standard cornmeal media at 25°C in a 12h light/dark cycle, unless for ageing experiments where flies were kept in 15% yeast/sugar media.<sup>28–30</sup> Strains used were *Oregon R*, *W<sup>1118</sup>*, *nSyb-gal4* (a kind gift from Dr Sean Sweeney), *TH-gal4*,<sup>31</sup> *UAS-EGFP*, *UAS-WT- $\alpha$ -syn-EGFP*.<sup>32</sup>

### Immunofluorescence

*Drosophila* larval neuromuscular junction (NMJ) dissections were carried out according to established protocol<sup>33</sup> and fixed either with 3.5% formaldehyde for 25 min or Bouin's fixative (Sigma) for 5 min. Primary antibodies used were anti-HRP (1:200—Immunochemicals 123–605–021), anti-CSP (1:200—DSHB), anti-Synapsin (1:50—DSHB), anti-nSynaptobrevin (1:150<sup>34</sup>; a kind gift from Dr Hugo Bellen, Baylor College of Medicine), anti-Synaptotagmin (1:1000<sup>91</sup>; a kind gift from Dr Sean Sweeney, University of York), anti-SNAP-25 (1:100<sup>35</sup>; a kind gift from Dr David Deitcher, Cornell University), anti-GFP (1:500—Thermo Fischer A6455), anti-BRP (1:50—DSHB). Adult CNS preparations were carried out as described previously.<sup>30</sup> The primary antibodies used were anti-TH (1:50—ImmunoStar) and anti-GFP (1:500—Thermo Fischer Scientific A6455). Secondary antibodies were Alexa fluor 488 and 568 (1:150; Invitrogen); for details see [Supplementary material](#).

### Imaging and analysis

Z-stacks of NMJ synapses innervating muscle 6/7 of Segment 3 were captured with a Nikon A1R confocal or Leica TCS SP5 microscopes. The adult *Drosophila* brain images were acquired using Nikon A1R confocal for DA neuron cluster analysis. The instant super resolution structured illumination microscopy (iSIM) was performed using Nikon Eclipse Ti-E Inverted microscope to image both for adult CNS and NMJ preparations.

For the fluorescence quantification, to build up the ratio between GFP signal in the synaptic boutons and axons, the intensity of 10 synaptic boutons (labelled with

anti-CSP) and 10 axonal regions (positive for anti-HRP and negative for anti-CSP) were quantified per NMJ. Thus, each  $n$  number represents the average value obtained from the division of fluorescence intensity of synaptic boutons/axon in each NMJ. For fluorescence quantifications of Synapsin and CSP, z-stacks were obtained using identical settings for all genotypes with same z-axis spacing between them within the same experiment and optimized for detection without saturation of the signal.<sup>36</sup> Ten synaptic boutons were analysed per NMJ using the free hand tool from ImageJ (<http://imagej.nih.gov/ij/>), with each point in the graphs representing the average of 10 synaptic boutons/NMJ.

BRP puncta number were manually counted in z-stacks using ImageJ and the Cell Counter plugin to record the total number of puncta per NMJ. Synapse surface area was calculated by creating a mask around the HRP channel, that labels the neuronal membrane, using ImageJ thresholding and 3D object counter.<sup>36</sup> DA neurons were manually counted through z-stacks using Cell Counter plugin using the anti-TH staining and each hemisphere represents an  $n$  number.<sup>30</sup>

## Western blotting

*Drosophila heads.* Quantitative western blotting from adult fly heads were performed as previously published protocol.<sup>28</sup> The following primary antibodies were used: anti-Synapsin (1:500—DSHB 3C11), anti-Syntaxin (1:1000—DSHB 8C3), anti-GFP (1:1000—Thermo Fischer A6455), anti-beta actin (1:1000—Abcam Ab8227) and anti-beta tubulin (1:1000—DSHB E3). Secondary antibodies were IRDye 800 conjugated goat anti-rabbit (1:10 000, Rockland Immunochemicals) and Alexa Fluor 680 goat anti-mouse (1:10 000, Invitrogen). The  $n$  number correspond to independent biological replicate containing 5–10 fly heads/genotype (for details see [Supplementary material](#)).

## Analysis of neuronal function

The Steady State Visual Evoked Potential (SSVEP) assay measured the output of the photoreceptors and second-order lamina neurons using protocol described previously<sup>37</sup> (for details see [Supplementary material](#)).

## Behavioural analyses

### *Drosophila* Arousal Tracking system

*Drosophila* Arousal Tracking (DART) was used to perform single fly tracking of age-matched mated females using protocol described previously<sup>38,39</sup> (for details see [Supplementary material](#)).

### Startle-induced negative geotaxis

Startle-induced negative geotaxis (SING) was used to assess the locomotor ability of flies following a startle

stimulus to which flies display a negative geotaxis response (modified from Ruan et al.<sup>39</sup>). A group of 10 mated age-matched female flies, per genotype, were transferred into the experimental tubes. After the tubes of all genotypes tested being placed in custom-made apparatus, flies were allowed to acclimatise for 20 min. Control and experimental groups were always assayed together by tapping all the flies to the bottom of the tubes and allowing them to climb as a negative geotaxis response. After 10 s, the number of flies that successfully climbed above the 7 cm line was recorded. This assay was repeated five times allowing 1 min rest during between trials (for details see [Supplementary material](#)).

### Proboscis extension response—Akinesia assay

The proboscis extension response (PER) assay was performed as protocol described previously<sup>37</sup> (for details see [Supplementary material](#)).

## Human post-mortem tissue analysis

### Brain tissue samples

Detailed description of brain samples, diagnose criteria and neuropathological assessments have been previously published.<sup>40</sup> Brain tissue samples were provided from Brains for dementia research network. Consent for autopsy, neuropathological assessment and research were obtained and all studies were carried out under the ethical approval of the regional Ethical Review Board of Stockholm (2012/910–31/4). Thirty cases in total/brain regions were used for the western blot experiments. Controls were defined as subjects with no clinical history and no neuropathological evidence of a neurodegenerative condition.

### Quantitative western blotting

For western blot analysis, 500 mg of frozen tissue was homogenized in ice-cold buffer containing 50 mM Tris-HCL, 5 mM EGTA, 10 mM EDTA, protease inhibitor cocktail tablets and 2 mg/ml pepstatin A dissolved in ethanol:dimethyl sulfoxide 2:1 (Sigma). To minimize inter-blot variability, 20  $\mu$ g total protein/samples were loaded in each lane of each gel on 7.5–10% SDS-polyacrylamide gel and then transferred to nitrocellulose membrane (Immobilon-P, Millipore). After blocking, membranes were incubated with primary antibodies followed by HRP conjugated secondary antibody. The following primary antibodies were used: rabbit polyclonal anti-LIPRIN- $\alpha$ 3 (1:1000, Synaptic Systems 169 102); Rabbit anti-LIPRIN- $\alpha$ 4 (1:1000, Abcam—ab136305); Rabbit anti-GAPDH (1:5000, Abcam, ab22555). Secondary antibodies used were donkey anti-rabbit (1:10 000, Invitrogen NA9340V) or donkey anti-rabbit (1:5000, LICOR, 926–32213) (for details see [Supplementary material](#)).

## Statistical analysis

GraphPad Prism 8 was used to perform the statistical analyses. Comparison of means were performed using either *t*-test; one-way ANOVA or Kruskal–Wallis test followed by Dunnett’s, Tukey’s or Dunn’s multiple comparison *post hoc* tests. The significance was defined as  $P < 0.05$ , error bars are shown as SEM. For complete description, see [Supplementary material](#).

## Data availability

The data supporting the findings of this study are available within the article and in [Supplementary material](#).

## Results

### $\alpha$ -Syn accumulates in presynaptic terminals

To investigate the consequences of  $\alpha$ -syn accumulation on synapse structure and function, we used transgenic *Drosophila* to express human wild-type  $\alpha$ -syn fused to EGFP (*UAS-WT- $\alpha$ -syn-EGFP*) alongside with control animals expressing EGFP only (*UAS-EGFP*).<sup>32</sup> This genetic model is an invaluable tool to investigate the toxic gain-of-function of  $\alpha$ -syn as the *Drosophila* genome lacks a homologue of the SNCA gene.<sup>41</sup> We first compared the expression pattern of  $\alpha$ -syn with the respective EGFP control by using the pan-neuronal driver *nSyb-Gal4*. Using immunohistochemistry, the localization and the expression pattern of  $\alpha$ -syn were determined at the *Drosophila* L3 larval NMJ by colocalization with cysteine string protein (CSP) and horseradish peroxidase (HRP) (Fig. 1A and B). CSP labels boutons containing synaptic vesicles at the presynaptic terminal<sup>42,43</sup> while HRP labels synaptic membranes<sup>44</sup> (Fig. 1A). The control expressing EGFP only and the experimental group expressing  $\alpha$ -syn-EGFP displayed co-localization with CSP (Fig. 1B). In addition, EGFP and  $\alpha$ -syn were also detectable in axonal domains labelled with anti-HRP and devoid of synaptic boutons, however, the EGFP expression pattern in these areas was very distinct between control and experimental group (Fig. 1B and C, arrowheads and dashed boxes).  $\alpha$ -syn immunolabelling was enriched in regions with a high density of synaptic boutons. In order to quantify this phenotype, EGFP intensity was measured in regions of CSP-positive synaptic boutons, and in CSP-negative axonal regions, in both control and experimental conditions. A ratio of EGFP intensity was calculated by dividing the values obtained from synaptic boutons by values obtained from axonal regions. Values  $\sim 1$  indicated that EGFP intensity is similar in the two regions while values higher than 1 identified a higher EGFP intensity in synaptic boutons compared with axonal regions. The analysis revealed

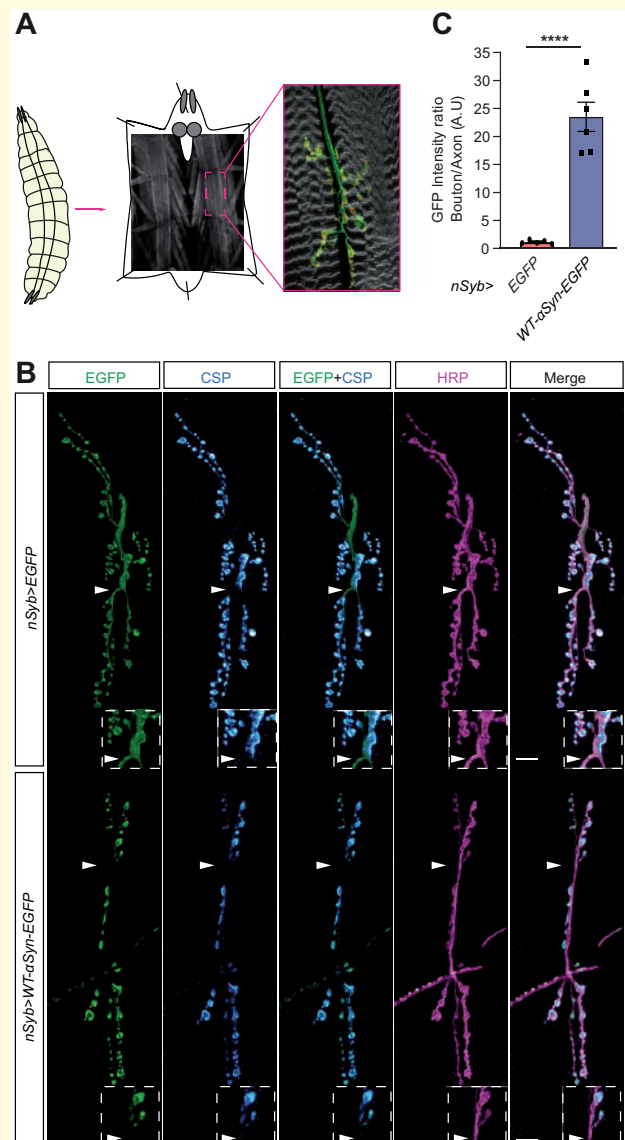


**Figure 1**  $\alpha$ -Syn accumulates in synaptic boutons at the *Drosophila* NMJ. (A) Third instar larval stage (L3) *Drosophila* (left) was used to investigate presynaptic terminals (*boutons*) terminating at the NMJ (middle). Immunohistochemistry assay reveals the muscle fibres (grey) stained with phalloidin that binds to actin; the axons descending from the motor neuron and terminating onto the muscles are labelled with anti-HRP (green); and the presynaptic terminal of the motor neuron labelled with anti-BRP (red). (B) Representative image of NMJ of *nSyb>EGFP* and *nSyb>WT- $\alpha$ -syn-EGFP* larvae immunostained with anti-GFP (green), anti-CSP (cyan) and anti-HRP (magenta). Arrowheads indicate accumulation of WT- $\alpha$ -syn-EGFP in synaptic boutons, which are immunolabelled with anti-CSP while control EGFP is homogeneously expressed in synaptic boutons and axonal regions devoid of CSP immunoreactivity; dashed boxes show a higher magnification of the areas indicated by the arrowheads. (C) Quantitative analysis of the ratio of GFP fluorescence intensity between boutons and axons; \*\*\*\* $P = 0.0001$ ; mean  $\pm$  SEM shown for each genotype ( $n = 5-6$  flies/genotype). Statistical analyses were performed using unpaired two-tailed *t*-test. Scale bars: 10  $\mu$ m.

that  $\alpha$ -syn immunofluorescence was significantly higher in synaptic boutons than in axons compared with the control NMJ expressing EGFP only (Fig. 1B and C; Supplementary Table 1, arrowheads and dashed boxes). These data suggest that  $\alpha$ -syn accumulates predominantly in presynaptic terminals and to a lesser extent in axonal areas devoid of synaptic boutons in the NMJ.

## Accumulation of $\alpha$ -syn affects presynaptic proteins

Previous studies demonstrated that the levels of synaptic proteins are altered in patients with Parkinson's disease and related disorders,<sup>24,25</sup> however, it is unclear whether and how  $\alpha$ -syn accumulation might be related to the disease. We, therefore, investigated whether presynaptic accumulation of  $\alpha$ -syn leads to alterations in the expression and/or localization of presynaptic proteins that are essential for neurotransmission. We first used the larval L3 NMJ to evaluate the effect of  $\alpha$ -syn accumulation on synaptic vesicle proteins CSP and Synapsin, the SNARE complex proteins, SNAP-25 and Synaptobrevin, and the synaptic vesicle-specific  $\text{Ca}^{2+}$ -binding protein Synaptotagmin.

CSP is a synaptic vesicle protein whose loss-of-function in *Drosophila* causes synaptic degeneration and

lethality.<sup>45,46</sup> CSP acts as a chaperone in the presynaptic terminal<sup>47,48</sup> and has been shown to be altered in Parkinson's disease patients as well as in cellular models inoculated with pre-formed fibrils of  $\alpha$ -syn.<sup>25,49</sup> We measured the expression levels and localization of CSP at the larval NMJ by immunofluorescence, which revealed that CSP levels but not its localization were downregulated in synaptic boutons co-labelled with  $\alpha$ -syn when compared with EGFP controls (Fig. 2A). Quantification of mean fluorescence intensity was performed as a proxy for expression level in single synaptic boutons revealed significantly reduced CSP levels in larvae expressing  $\alpha$ -Syn compared with controls expressing EGFP only (Fig. 2B; Supplementary Table 1).

We next examined the presynaptic protein Synapsin which is associated with the cytoplasmic surface of the synaptic vesicle membrane and plays a fundamental role in regulating vesicle trafficking.<sup>50–52</sup> We measured Synapsin fluorescence intensity and localization in single synaptic boutons of larvae expressing either EGFP as control or  $\alpha$ -syn (Fig. 2C). Quantitative analysis of Synapsin fluorescence intensity revealed that  $\alpha$ -syn accumulation caused a reduction in Synapsin expression levels in synaptic boutons, compared with the control group (Fig. 2D; Supplementary Table 1); however, alterations in Synapsin localization were not observed. In contrast to

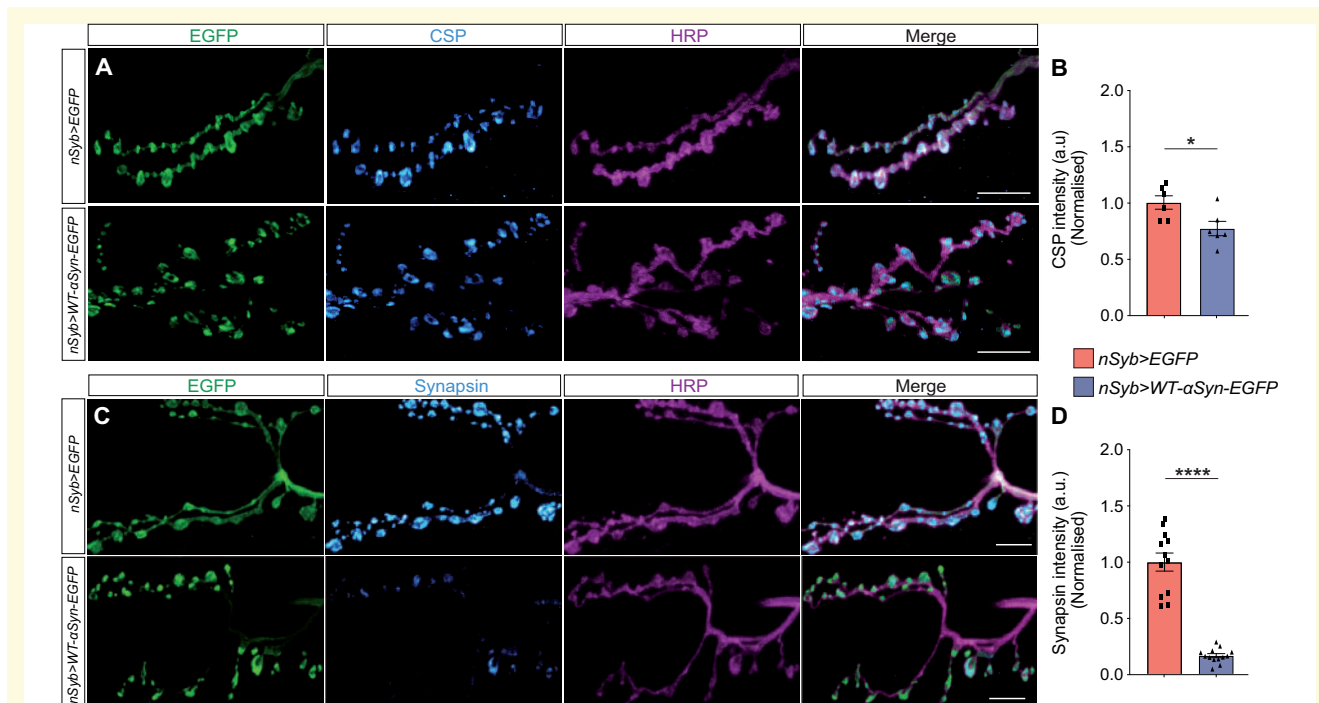


**Figure 2** Accumulating  $\alpha$ -syn downregulates presynaptic proteins. **(A)** Confocal images of NMJ immunolabelled with anti-CSP, anti-GFP and anti-HRP. **(C)** Confocal images of NMJ staining with anti-Synapsin, anti-GFP and anti-HRP. **(B)** Quantitative analysis of the fluorescence levels of CSP revealed downregulation in the NMJ of *nSyb>WT- $\alpha$ -syn-EGFP* larvae compared with control; \* $P = 0.0248$ ; mean  $\pm$  SEM shown for each genotype ( $n = 6$  flies/genotype). **(D)** Quantitative analysis of the Synapsin fluorescence levels showed downregulation in the NMJ of *nSyb>WT- $\alpha$ -syn-EGFP* larvae compared with control; \*\*\*\* $P < 0.0001$ ; mean with SEM shown for each genotype ( $n = 12$ –13 flies/genotype). Statistical analyses were performed using unpaired two-tailed *t*-test. Scale bars: 10  $\mu$ m.

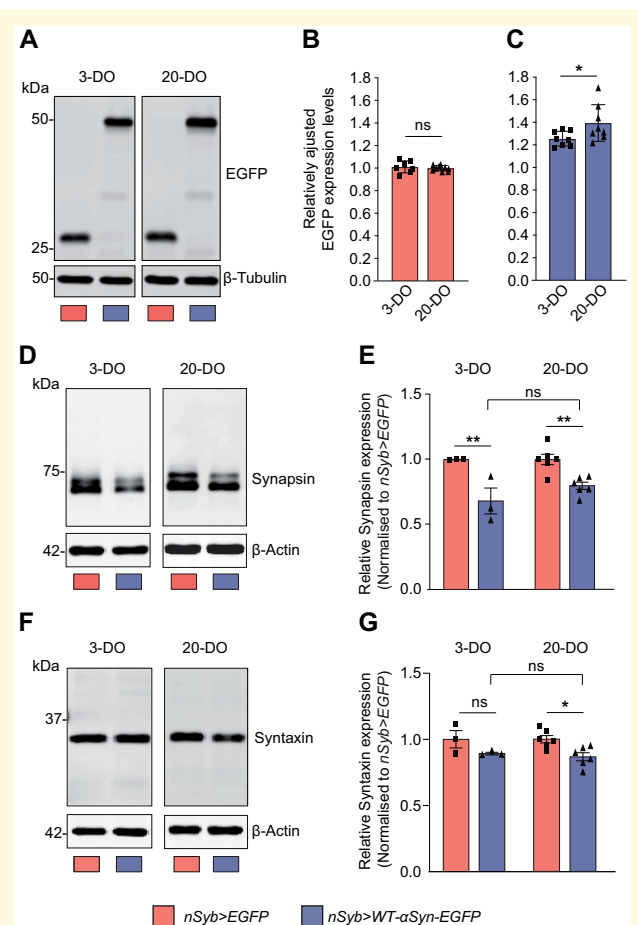


**Figure 3 Progressive accumulation of  $\alpha$ -syn affects presynaptic proteins in ageing animals.** (A–C) Expression levels of WT- $\alpha$ -syn-EGFP expressed under the control of pan-neuronal driver *nSyb-Gal4* increased at 20 days of age compared with the levels observed in fly brains at 3 days of age; \* $P=0.0411$ , ns—not significant  $P>0.05$ ,  $n=7-9$ . Such accumulation was specific for WT- $\alpha$ -syn-EGFP since the control flies expressing EGFP only (A, B) showed no alteration in the expression levels of EGFP. (D, E) The expression levels of the synaptic vesicle protein Synapsin were reduced in flies expressing WT- $\alpha$ -syn-EGFP at Day 3 (\*\* $P=0.0024$ ) and 20 (\*\* $P=0.0056$ ) compared with control flies;  $n=3-6$ . (F, G) The expression levels of Syntaxin, a protein of the presynaptic SNARE complex, also had its levels reduced at Day 20 in fly brain expressing WT- $\alpha$ -syn-EGFP compared with control; \* $P=0.0151$ , ns—not significant  $P>0.05$ ,  $n=3-6$ . Mean  $\pm$  SEM are shown, statistical analyses were performed using unpaired two-tailed *t*-test. Full uncropped blots are available in [Supplementary material](#).

Fig. 3B; Supplementary Table 1), levels of  $\alpha$ -syn were increased over time (\* $P=0.0411$ ; Fig. 3C; Supplementary Table 1). We then assessed the levels of Synapsin and Syntaxin in adult flies, which revealed downregulated Synapsin levels at Day 3 and 20 (3-DO: \*\* $P=0.0024$ ; 20-DO: \*\* $P=0.0056$ ; Fig. 3D and E; Supplementary Table 1), similar to the phenotype observed in synaptic boutons of the NMJ. The expression levels of Syntaxin, a component of the SNARE complex<sup>53</sup>, were reduced at Day 3 but only significantly downregulated at Day 20 when compared with control (3-DO:  $P=0.2079$ ; 20-DO: \* $P=0.0151$ ; Fig. 3F and G; Supplementary Table 1). Together, these findings indicate that  $\alpha$ -syn accumulates in the *Drosophila* brain, which in turn causes specific alterations of presynaptic proteins, with CSP, Syntaxin and Synapsin being especially susceptible to the deleterious effects of accumulating  $\alpha$ -syn.

### Presynaptic accumulation of $\alpha$ -syn reduces AZ density

Given the impact of  $\alpha$ -syn on presynaptic proteins, we investigated whether the accumulation of  $\alpha$ -syn may alter the AZ in *Drosophila*. The AZ is a specialized presynaptic site required for vesicle docking and neurotransmitter exocytosis, conveying speed and accuracy to synaptic transmission.<sup>54-56</sup> We used confocal and instant structured iSIM to NMJs labelled with anti-Bruchpilot (BRP) (Fig. 4A and B). BRP encodes a cytoskeletal protein essential for the structural integrity and the function of electron-dense projection (T-bar) at the AZ.<sup>57,58</sup>

Expression and accumulation of  $\alpha$ -syn in *nSyb>WT- $\alpha$ -syn-EGFP* L3 larvae caused a reduction in the total number of BRP-labelled AZ puncta compared with control groups *nSyb/+* and *nSyb>EGFP* (versus *nSyb/+* \* $P=0.0189$ ; versus *nSyb>EGFP* \* $P=0.0492$ ; Fig. 4C; Supplementary Table 1). A detailed analysis accounting also for the surface area of the NMJ labelled by anti-HRP,<sup>59</sup> revealed also a significant reduction in the total number of puncta in *nSyb>WT- $\alpha$ -syn-EGFP* larvae, when compared with controls (versus *nSyb/+* \* $P=0.0289$  and *nSyb>EGFP* \* $P=0.03$ ; Fig. 4D; Supplementary Table 1). In contrast, neither the total number of synaptic boutons (versus *nSyb>EGFP*  $P=0.2976$ ; Fig. 4E; Supplementary Table 1) nor the morphology and the localization of BRP puncta (Fig. 4B, dashed lines) were affected. Together these data demonstrate that accumulation of  $\alpha$ -syn alters the AZ of presynaptic terminals.

### $\alpha$ -Syn accumulation impairs neuronal function

The core function of BRP is the maintenance of the presynaptic AZ and thus synaptic homeostasis and function.<sup>57</sup> The observed reduction of BRP-positive puncta suggested that physiological defects could occur as a result of presynaptic accumulation of  $\alpha$ -syn. To

CSP and Synapsin, we did not observe any changes in fluorescence intensity levels and localization of SNAP-25, Synaptobrevin or Synaptotagmin (Supplementary Fig. 1).

To examine the progression of  $\alpha$ -syn-mediated presynaptic deficits, we assessed  $\alpha$ -syn accumulation in adult flies at Day 3 and 20 and performed western blots of heads of flies expressing  $\alpha$ -syn or EGFP (Fig. 3A–C). While the levels of EGFP were unchanged ( $P=0.5777$ ;



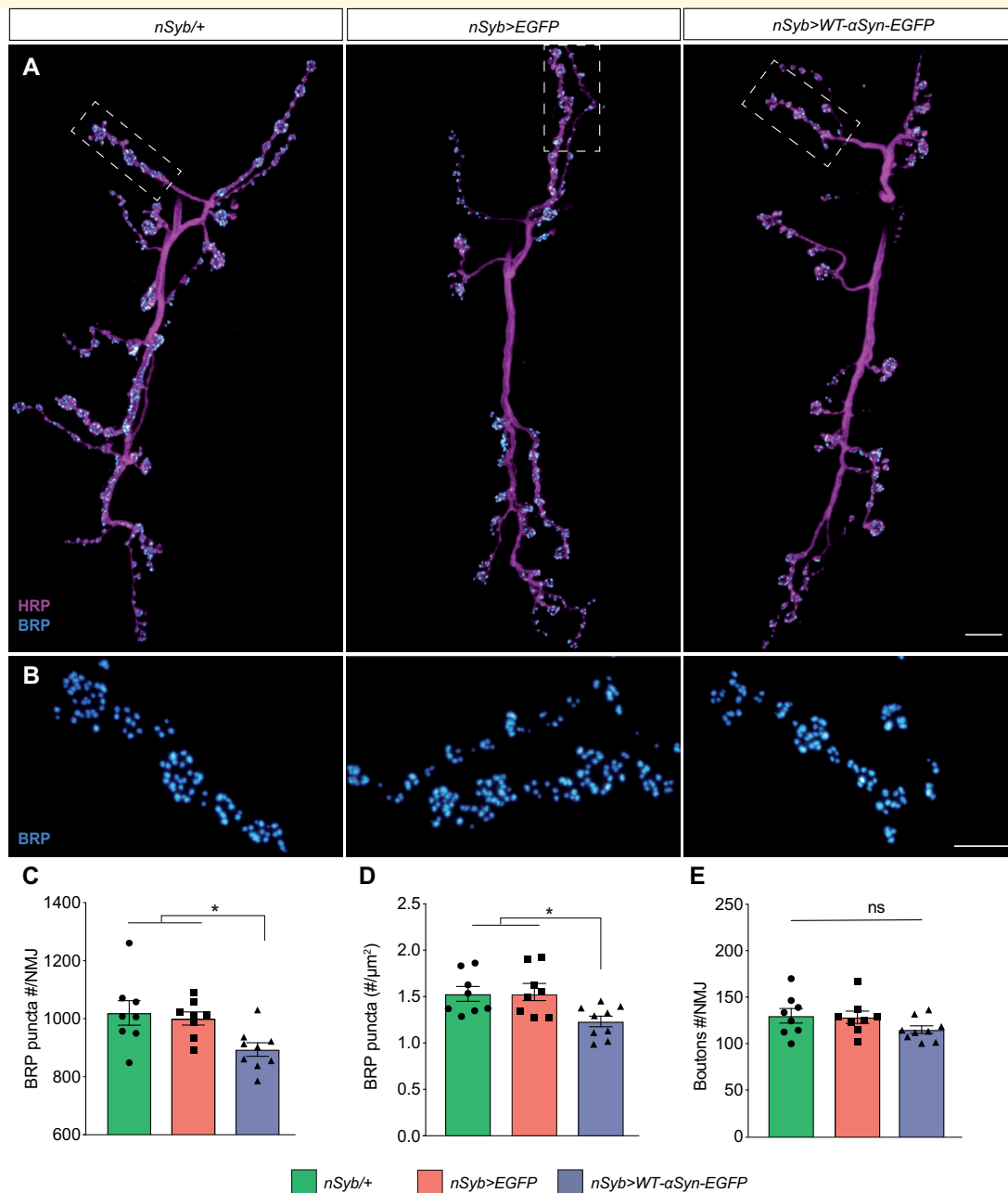


**Figure 4 Presynaptic active zones are reduced by accumulating  $\alpha$ -syn.** (A) Confocal images of NMJ, immunolabelled with anti-nc82/BRP and anti-HRP. (B) Dashed box represents the section of the NMJ (A) imaged with instant super resolution structured iSIM. (C) Quantitative analysis of total number of BRP puncta that represents the AZs labelled with anti-nc82/BRP per NMJ;  $*P = 0.0189$  compared with *nSyb/+* and  $*P = 0.0492$  compared with *nSyb>EGFP*. (D) Number of BRP puncta normalized by the synaptic surface micrometres square immunolabelled with anti-HRP;  $*P = 0.0289$  compared with *nSyb/+* and  $*P = 0.03$  compared with *nSyb>EGFP*. (E) The total number of synaptic boutons/NMJ was unchanged. All graphs are represented as mean  $\pm$  SEM shown for each genotype ( $n = 8$  flies for *nSyb/+* and *nSyb>EGFP*; and nine flies for *nSyb>WT- $\alpha$ -syn-EGFP*). Statistical analyses were performed using one-way ANOVA test followed by Tukey's multiple comparison *post hoc* test. Scale bars: (A) 10  $\mu$ m and (B) 5  $\mu$ m.

investigate whether synaptic efficacy and neurotransmission were affected, we determined the SSVEP in adult flies (Fig. 5). The SSVEP quantifies the physiological response to flickering stimuli which generate frequency- and phase-locked response components with a very high signal-to-noise ratio (Fig. 5A–C).<sup>37,60</sup> In *Drosophila*, the

net response of flickering stimuli is mediated by retinal photoreceptor cells together with lamina and medulla neurons that are electrically linked (Fig. 5C and D).<sup>62</sup> The visual response negatively correlates with dopamine levels in the brain,<sup>63</sup> with dopamine required to inhibit the response to visual stimuli.<sup>60</sup>

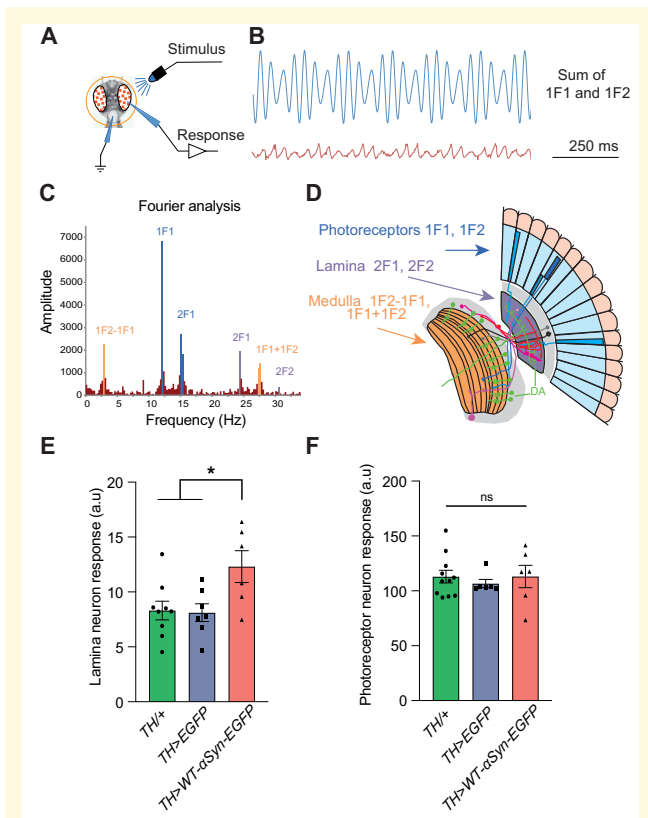


**Figure 5**  $\alpha$ -Syn accumulation in dopaminergic neurons impairs visual response. (A) Steady-state visual evoked potential (SSVEP) was measured in flies raised in the dark and restrained in a Gilson pipette tip. The recording electrode was placed on the surface of the eye, with a reference electrode in the mouthparts. A full field blue light stimulus is provided from an LED. A pattern of 45 stimuli is provided, with different amounts of the 1F1 (12 Hz) and 2F1 (15 Hz) stimuli. (B) An example stimulus made up of 70% contrast at 1F1, and 30% contrast at 2F1 and its response. (C) The response (in B) is analysed by the Fast-Fourier Transform, revealing that the visual system responds to the supplied frequencies (1F1, 2F1) but also to their multiples (2F1, 2F2) and to the sums and differences (1F1 + 1F2; 1F2 - 1F1). Higher frequency harmonics are also seen, notably 2F1 + 2F2. (D) Genetic dissection<sup>60,61</sup> shows that the majority of the 1F1 and 1F2 components come from the photoreceptors, the 2F1 and 2F2 come from the lamina neurons, and the 1F1 + 1F2, 1F1 + 1F2 and 1F2 - 1F1 from the medulla. (A–D) Modified after Afsari et al.<sup>60</sup> and Petridi et al.<sup>37</sup> (E) Flies expressing WT- $\alpha$ -Syn-EGFP under control of *TH-Gal4* driver demonstrated a higher lamina neuron activity in the SSVEP, which is known to negatively correlate with levels of dopamine in the brain; \* $P=0.03$ . (F) Photoreceptors of *TH>WT- $\alpha$ -Syn-EGFP* displayed no alteration in their response compared with control groups; ns—not significant  $P>0.05$ ,  $n=6-11$  flies/genotype. Mean  $\pm$  SEM are shown, statistical analyses were performed using one-way ANOVA with Tukey's multiple comparison *post hoc* test.

Our analysis revealed that lamina neurons in 3-day-old *TH>WT- $\alpha$ -syn-EGFP* flies showed an increased SSVEP response upon stimulation when compared with control groups (versus *TH/+* \* $P=0.0313$ ; versus *TH>EGFP*

\* $P=0.0325$ ; Fig. 5E; Supplementary Table 1). This response was specific to lamina neurons, as photoreceptor cells showed no alteration in their SSVEP response (versus *TH/+*  $P=0.9998$ ; versus *TH>EGFP*  $P=0.8261$ ; Fig. 5F; Supplementary Table 1). The difference in stimuli response between the lamina and photoreceptor neurons correlated well with the far more extensive DA innervation in the lamina than the photoreceptor layer (Fig. 5D).<sup>37,60</sup> Because dopamine inhibits the SSVEP response,<sup>60</sup> these data suggest that *TH-Gal4* driven accumulation of  $\alpha$ -syn in DA neurons impaired synaptic output of DA-rich lamina neurons, thereby reducing their visual response inhibition which in turn resulted in an increased SSVEP response.

## Accumulation of $\alpha$ -syn progressively impairs motor behaviour

Parkinson's disease patients suffer from a variety of motor symptoms ranging from resting tremor to bradykinesia and akinesia, related to the reduction of striatal dopamine.<sup>64</sup> However, these symptoms only become clinically apparent when a large proportion of DA neurons have already been lost.<sup>5</sup> We, therefore, investigated whether the accumulation of  $\alpha$ -syn and in turn the alterations in presynaptic proteins would cause any motor deficits in adult flies. We employed three independent assays to quantify voluntary and reflexive motor behaviour, the DART system,<sup>38</sup> startle-induced negative geotaxis (SING)<sup>30,65</sup> and the proboscis extension response (PER).<sup>66</sup>

We specifically targeted  $\alpha$ -syn to DA neurons and first determined anti- $\alpha$ -syn immunoreactivity in the adult brain of *TH>WT- $\alpha$ -syn-EGFP* flies compared with *TH>EGFP* controls. Anti- $\alpha$ -syn antibody staining was detectable in DA cell bodies, their neuronal projections and in synaptic terminals (Supplementary Fig. 2A–L). Next, we measured their spontaneous motor activity with DART at 3 and 20 days of age (Fig. 6A). The activity and speed of *TH>WT- $\alpha$ -syn-EGFP* flies was greatly impaired at Day 3 (Fig. 6B and C; Supplementary Table 1) compared with control flies *TH-Gal4/+* and *WT- $\alpha$ -syn-EGFP/+*. Notably, both activity and speed were further reduced in flies accumulating  $\alpha$ -syn compared with controls at Day 20 (Fig. 6B and C; Supplementary Table 1). To better understand the detrimental impact of  $\alpha$ -syn on movement patterns, we decomposed and analysed movement as units. The first unit comprised the initiation of a motor action (Fig. 6D, red arrows), the action initiation; the second unit was the bout length, depicting for how long the flies maintain a bout of activity (Fig. 6D, dark grey boxes); and the third unit was the inter-bout interval that quantifies the duration of the pause between the end of a previous and the beginning of a new bout of activity (Fig. 6D, white boxes). These units were collectively named activity metrics.

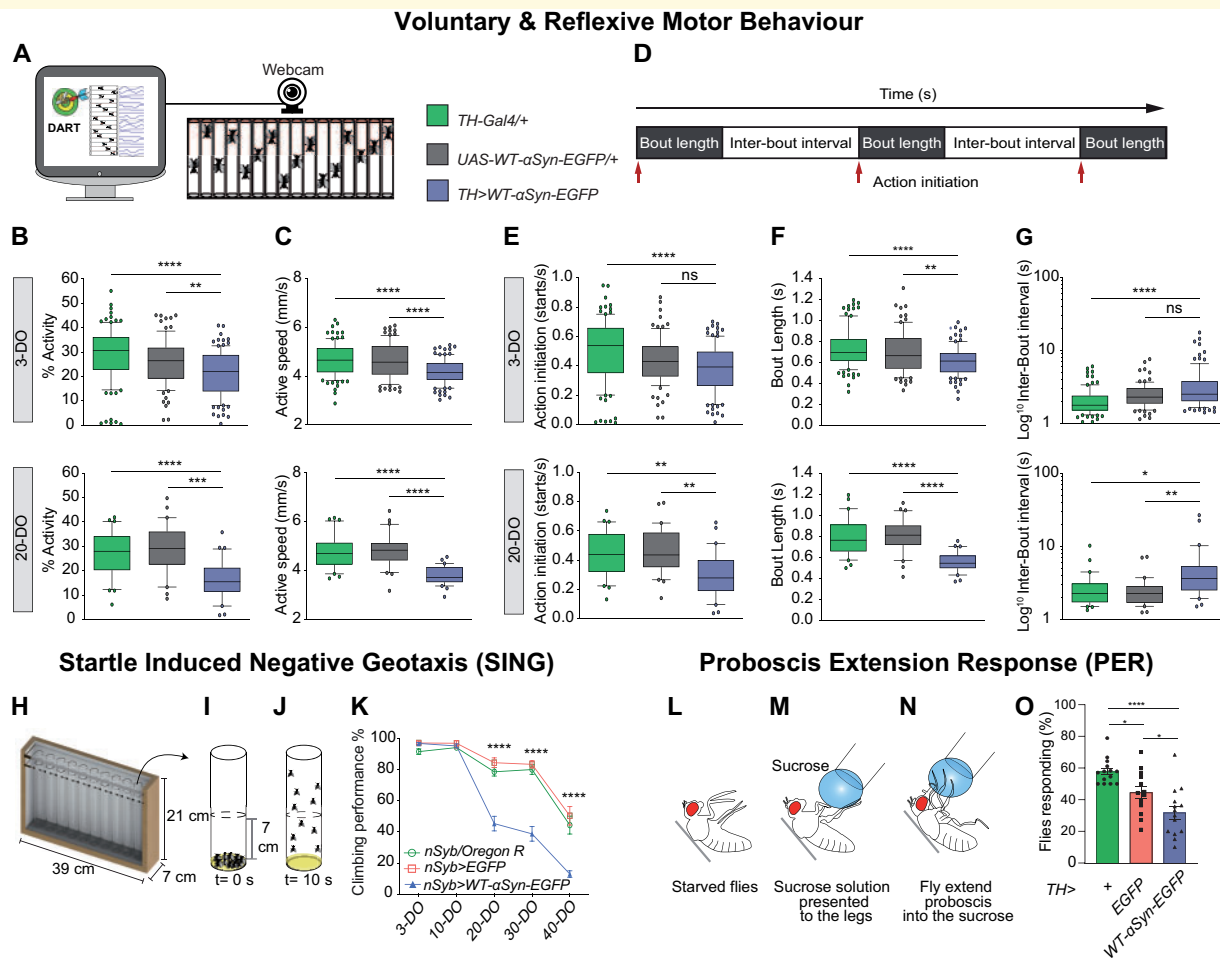


**Figure 6 Synaptopathy induced by  $\alpha$ -syn accumulation causes progressive motor impairment and akinetic behaviour prior to age-related dopaminergic neurodegeneration.**

(A) The DART system was used to measure spontaneous activity of individual flies that were continuously recorded at five frames per second for 2 h, as set by the DART software using a USB-webcam. (B) *Top*: spontaneous activity is reduced in 3-day-old flies (3-DO) expressing WT- $\alpha$ -syn-EGFP compared with controls;  $****P < 0.0001$ ,  $**P = 0.0071$  ( $n = 90$ –100 flies/genotype). *Bottom*: spontaneous activity is further reduced in 20-day-old (20-DO) TH>WT- $\alpha$ -syn-EGFP when compared with controls;  $****P < 0.0001$  and  $**P = 0.0002$  ( $n = 30$  flies/genotype). (C) Active speed of 3-day-old flies (3-DO) (*top*) and 20-day-old flies (20-DO) (*top*) is impaired by WT- $\alpha$ -syn-EGFP expression;  $****P < 0.0001$ . (D) Schematic of the activity metrics units. The initiation of a locomotor action (red arrows) is called action initiation. Bout length is the length of a motor action (dark grey boxes); and the pause between the end and beginning of a new motor action is called inter-bout interval (white boxes). (E) *Top*: the number of locomotor actions initiated by 3-day-old (3-DO) TH>WT- $\alpha$ -syn-EGFP flies was reduced compared with the control group TH/+;  $****P < 0.0001$  and ns—not significant. *Bottom*: the locomotor actions initiated by 20-day-old (20-DO) TH>WT- $\alpha$ -syn-EGFP flies was reduced when compared with both controls;  $**P < 0.0011$  compared with TH/+ and  $**P = 0.0097$  compared with WT- $\alpha$ -syn-EGFP/+ control. (F) The length of each bout of activity was shorter in TH>WT- $\alpha$ -syn-EGFP flies at 3 (*top*) and 20 (*bottom*) days of age, depicting their impaired ability of sustaining a locomotor action;  $**P = 0.0053$ ;  $****P < 0.0001$ . (G) The length between each bout of activity was longer in flies expressing WT- $\alpha$ -syn-EGFP at 3 (*top*) and 20 (*bottom*) days;  $*P = 0.0108$ ,  $**P < 0.0014$ ,  $****P < 0.0001$ . Box-and-whisker plots represent the median (horizontal line), 25 and 75% quartiles (box), and 5 and 95% quartiles (whiskers); statistical analyses were performed using Kruskal–Wallis test with Dunn’s multiple comparison *post hoc* test. (H) Custom-made apparatus used to perform startle induced negative geotaxis (SING) assay which allows all fly genotypes to be probed under equal conditions simultaneously. (I) A group of 10 flies were placed in an assay tube containing 1 cm of fresh media and then allocated back in the fly holder. Next, the holder was gently tapped allowing all the flies to reach the bottom of the tubes ( $t = 0$  s). (J) After 10 s, the number of flies that successfully climbed above the 7 cm line is recorded. (K) Cohorts of flies were analysed at 3, 10, 20, 30 and 40 days of age. The analysis showed an age-related deficiency in their climbing performance which was further enhanced by the overexpression of WT- $\alpha$ -syn-EGFP;  $****P < 0.0001$ ; mean  $\pm$  SEM are shown,  $n = 9$ –13 groups of 10 flies. PER assay evaluated the ability of flies to respond to sucrose offer after starvation. (L) Flies were fixed in a card (grey bar) with rubber cement and were left to recover for 3 h. (M) Starved flies were presented with a droplet of 100 mM of sucrose to the legs and then immediately scored; (N) flies that extended or not their proboscis in response to sucrose were scored. (O) Young flies (5–8-day-old) expressing WT- $\alpha$ -syn-EGFP under control of TH-Gal4 driver showed a reduced response to sucrose compared with controls flies, resembling an akinetic behaviour;  $*P = 0.03$  and  $****P < 0.0001$ ; mean  $\pm$  SEM shown for each genotype ( $n = 13$ –14 flies/genotype).

DA-specific expression of  $\alpha$ -syn altered activity metric parameters in 3-day-old flies (Fig. 6E–G, top; Supplementary Table 1). Three-day-old *TH>WT- $\alpha$ -syn-EGFP* flies revealed a reduced ability to initiate locomotor movements compared with *TH/+* controls (Fig. 6E, top). In addition, *TH>WT- $\alpha$ -syn-EGFP* flies showed a marked impairment in the capacity to maintain a motor action, thus showing shorter bouts of activity (Fig. 6F, top). Furthermore, these flies also displayed a longer interval between each activity bout (Fig. 6G, top). These alterations were also observed in 20-day-old *TH>WT- $\alpha$ -syn-EGFP* flies when compared with controls (Fig. 6E–G). Together these data demonstrate that expression of  $\alpha$ -syn in DA neurons caused an early onset of abnormalities that affected spontaneous motor activity, exemplified by shorter bouts of activity with reduced speed and separated by longer pauses.

To investigate the impact of  $\alpha$ -syn mediated motor impairment over an extended period of time, we utilized the SING assay which probes the ability of flies to climb to the top of a tube after being gently tapped to the bottom<sup>67,68</sup> (Fig. 6H–J). Independent cohorts of flies either expressing *UAS-WT- $\alpha$ -syn-EGFP* or *UAS-EGFP* were aged and tested at 3, 10, 20, 30 and 40 days old for their SING behaviour. *nSyb>WT- $\alpha$ -syn-EGFP* flies showed a severe reduction in their climbing ability starting at Day 20 compared with both control groups (Fig. 6K; Supplementary Table 1). This phenotype worsened as the flies reached 30 and 40 days of age, respectively (Fig. 6K; Supplementary Table 1). These data demonstrate that accumulation of  $\alpha$ -syn and in turn alterations in presynaptic proteins lead to progressive motor deficits in ageing *Drosophila*.

To further investigate the impact of  $\alpha$ -syn expression on DA neuron function, we quantified the PER which is modulated by a single DA neuron, the TH-VUM cell.<sup>69</sup> PER behaviour measures the proboscis extension response of flies to sugar stimuli after a short period of starvation (Fig. 6L–O).<sup>66</sup> PER analysis showed the proportion of *TH>WT- $\alpha$ -syn-EGFP* flies responding to sugar stimuli was significantly lower compared with *TH/+* and *TH>EGFP* controls (Fig. 6O; Supplementary Table 1). This data demonstrate that  $\alpha$ -syn impairs the neural response to sugar stimuli, most likely because the activity of TH-VUM neuron is diminished. Thus, indicating that impaired dopamine signalling causes akinetic behaviour in *Drosophila*.

## $\alpha$ -Syn-induced synaptopathy causes DA neurodegeneration

The synaptopathy hypothesis suggests that synaptic dysfunction and the resulting behavioural deficits precede degenerative cell loss. To test this hypothesis, we aged *TH>WT- $\alpha$ -syn-EGFP* and control flies and quantified DA neuron numbers in specific clusters of the ageing *Drosophila* brain that were identified by

immunofluorescence with anti-tyrosine hydroxylase (TH) antibody.<sup>30</sup> We counted anti-TH-labelled DA neurons of PPL1 and PPL2, PPM1/2 and PPM3 clusters in the adult brain of 3, 20 and 40-day-old flies (Fig. 7A). At 3 days of age, *TH>WT- $\alpha$ -syn-EGFP* flies showed no significant loss of DA neurons in the PPL1 cluster compared with the control groups (Fig. 7B and C; Supplementary Table 1). At 20-day-old, analysis of *TH>WT- $\alpha$ -syn-EGFP* flies revealed a significant loss of DA neurons compared with controls (Fig. 7B and C; Supplementary Table 1), which was also observed in 40-day-old flies compared with age-matched controls (Fig. 7B and C; Supplementary Table 1). Similar to PPL1, analysis of the PPM3 cluster revealed a discrete loss of DA neurons at Day 20 when compared with *TH>EGFP* control and *TH/+* control at Day 40 (Fig. 7D; Supplementary Table 1). In contrast to PPL1 and PPM3, PPL2 and PPM1/2 clusters showed no significant alteration in the number of DA neurons over time due to WT- $\alpha$ -syn overexpression (Fig. 7E and F; Supplementary Table 1). Together these data demonstrate that  $\alpha$ -syn accumulation causes region-specific and progressive degeneration of DA neurons in the ageing brain of *Drosophila*.

## AZ protein is downregulated in human synucleinopathies

Our findings so far indicate that presynaptic  $\alpha$ -syn accumulation caused AZ deficits that resulted in decreased neuronal function and behavioural deficits in ageing *Drosophila* that occurred prior to progressive neurodegeneration. To evaluate the clinical significance of these *in vivo* findings, we examined whether AZ proteins were also altered in patient brain. For this, we re-analysed our previously published proteomics data that compared 32 post-mortem human brains in the prefrontal cortex of patients with PDD, DLB, Parkinson's disease and older adults without dementia.<sup>40</sup> Our previous analysis identified alterations in synaptic proteins that correlated with the rate of cognitive decline and reliably discriminated PDD from Alzheimer's disease patients.<sup>40</sup> Here we focussed on proteins enriched in the mammalian presynaptic AZ, including homologs of the RIM, PICCOLO, ELKS and LIPRIN- $\alpha$  protein families (Supplementary Table 2). Our initial analysis indicated potential alterations in AZ protein levels in patient brain, in particular LIPRIN- $\alpha$  proteins (Supplementary Table 2).

Liprin- $\alpha$ 3 and 4 proteins of the mammalian AZ play crucial roles in synapse assembly and function.<sup>70</sup> In mammals, Liprin- $\alpha$ 3 is highly expressed in the brain while Liprin- $\alpha$ 4 has a lower abundance in the central nervous system.<sup>70</sup> To corroborate our proteomics data, we carried out quantitative western blotting analysis of LIPRIN- $\alpha$ 3 and 4 in post-mortem tissue of prefrontal cortex (BA9), anterior cingulate cortex (BA24) and parietal cortex (BA40) in control, PDD and DLB patient brain samples. The demographics and neuropathological characteristics

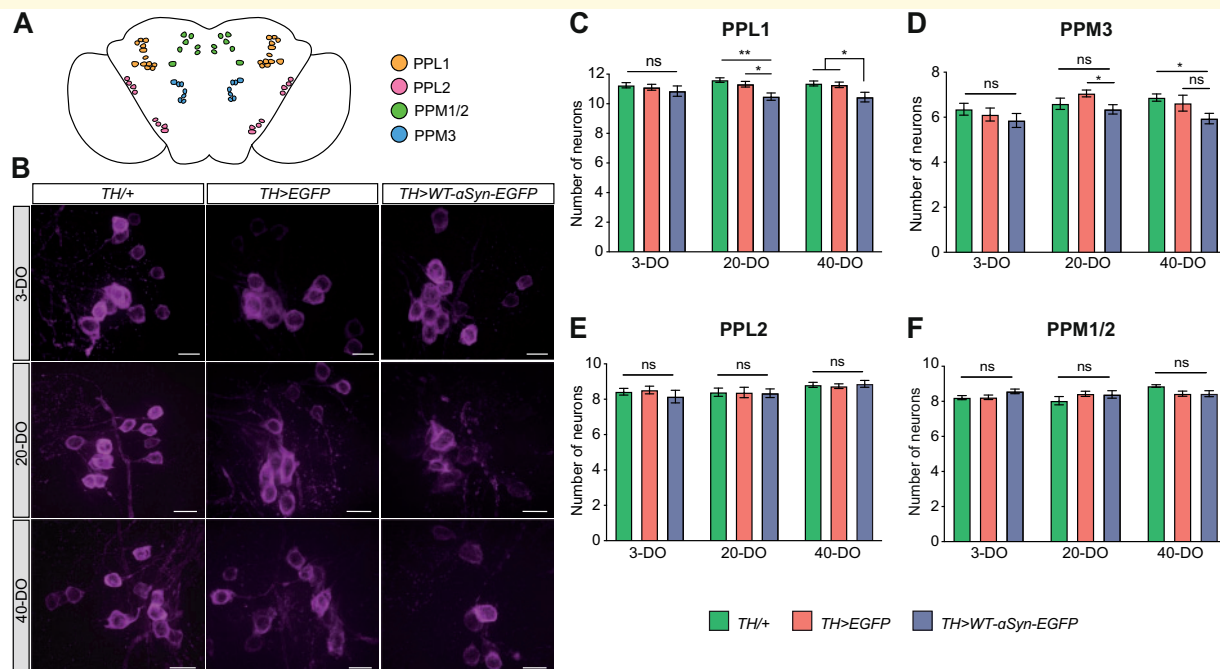


**Figure 7**  $\alpha$ -Syn-mediated synaptopathy causes progressive and age-related dopaminergic neurodegeneration. **(A)** Schematic depiction of dopaminergic (DA) neuron clusters in the adult *Drosophila* brain; paired posterior lateral 1 and 2 (PPL1 and PPL2), the paired posterior medial 1 and 2 (PPM1/2) and paired posterior medial 3 (PPM3). **(B)** Representative iSIM images from DA neurons from PPL1 clusters immunolabelled with anti-TH antibody. **(C)** Number of DA neurons per hemisphere from the PPL1 cluster is reduced at Day 20 and 40 compared with controls;  $**P = 0.0016$ ,  $*P = 0.0146$  for Day 20;  $*P = 0.0207$  compared with *TH/+*;  $*P = 0.0425$  compared with *WT- $\alpha$ -syn-EGFP/+* for Day 40. **(D)** PPM3 clusters displayed a discrete loss of DA neurons in *TH>WT- $\alpha$ -syn-EGFP* flies only when compared with *TH>EGFP* at Day 20 ( $*P = 0.0292$ ) and to *TH/+* at Day 40 ( $*P = 0.0333$ ). **(E, F)** DA neurons from PPL2 and PPM1/2 clusters were not affected by the expression of  $\alpha$ -syn;  $n = 22$ – $38$  hemispheres/genotype; ns—not significant  $P > 0.05$ . Mean  $\pm$  SEM shown, statistical analyses were performed using one-way ANOVA with Tukey's multiple comparison *post hoc* test. Scale bar =  $10 \mu\text{m}$ .

of the subjects included in our analysis are shown in [Supplementary Table 3](#). Levels of LIPRIN- $\alpha 3$  were unaltered in all brain regions evaluated from PDD and DLB when compared with controls ([Fig. 8A–C](#); [Supplementary Table 4](#)). In contrast, expression levels of LIPRIN- $\alpha 4$  were significantly downregulated in the prefrontal cortex of DLB patients compared with control patients ( $*P = 0.0349$ ; [Fig. 8B and C](#); [Supplementary Table 4](#)). On the other hand, no significant alteration was observed in cingulate cortex ( $P = 0.1192$ ) or in parietal cortex ( $P = 0.8737$ ; [Fig. 8B and C](#); [Supplementary Table 4](#)).

## Discussion

$\alpha$ -syn accumulation and aggregation is the defining pathogenic feature of Parkinson's disease and other synucleinopathies.<sup>3,5</sup>  $\alpha$ -syn pathology correlates with synaptic deficits and subsequent synaptopathy before neurons are lost.<sup>26,27,71</sup> However, the mechanisms and cascade of events underlying the pathogenic progression from  $\alpha$ -syn accumulation to synaptopathy and subsequent neurodegeneration are not well understood. Here we tested the hypothesis of  $\alpha$ -syn-mediated synaptopathy by expressing

the human wildtype form of  $\alpha$ -syn in *Drosophila*, a well-established model to study Parkinson's disease and synucleinopathy,<sup>41,72</sup> and monitored its effect over time in the ageing animal. Our findings indicate that targeted expression of human  $\alpha$ -syn leads to its accumulation in presynaptic terminals that caused downregulation of presynaptic proteins CSP, Synapsin and Syntaxin and a reduction in the number of AZ required for synaptic transmission. In addition to synaptic alterations,  $\alpha$ -syn accumulation caused impaired neuronal function and behavioural deficits leading to the progressive loss of DA neurons in ageing flies. While our approach of targeted  $\alpha$ -syn overexpression may relate more closely to familial forms of synucleinopathies, such as duplications and triplications of the encoding *SNCA* locus,<sup>73</sup> the observed data resemble key features of the onset and progression of Parkinson's disease, PDD and DLB, and demonstrate that accumulating  $\alpha$ -syn can cause synaptopathy and progressive neurodegeneration. Our findings imply that one, if not the first cytotoxic insult of  $\alpha$ -syn pathology, is its accumulation in presynaptic terminals, which impairs presynaptic AZs, a phenotype we also observed in post-mortem tissue of DLB patients. The resulting impaired synaptic efficacy and diminished neuronal function affect

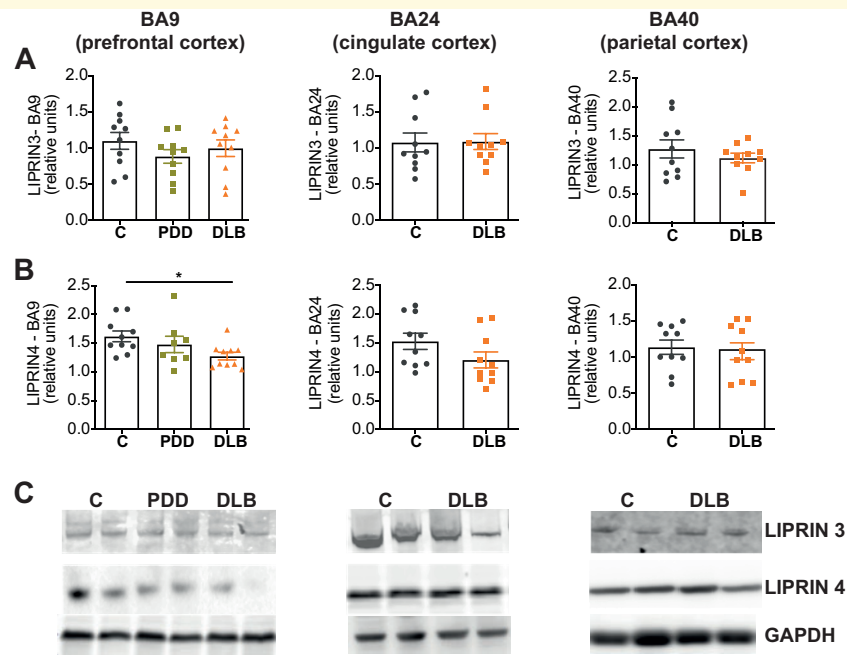


**Figure 8 Active zone protein is affected in human synucleinopathy.** (A, B) Quantitative western blots revealed no significant alteration in the expression levels of LIPRIN- $\alpha$ 3 in the prefrontal cortex (BA9), cingulate cortex (BA24) and parietal cortex (BA40), while LIPRIN- $\alpha$ 4 (B) was found to be downregulated in prefrontal cortex of DLB patients  $*P = 0.0389$ ; ( $n = 8-10$ ). (C) Representative images from the western blotting membranes. All graphs are represented as mean  $\pm$  SEM shown. Statistical analyses were performed using one-way ANOVA test followed by *post hoc* Dunnett's multiple comparison test. Full uncropped blots are available in [Supplementary material](#).

behavioural output, which over time leads to progressive neurodegeneration.

Our findings are in line with post-mortem studies where  $\alpha$ -syn was found as small aggregates in the pre-synaptic terminal.<sup>19,20</sup> Dendrites and spines of DLB patients with accumulation of aggregated  $\alpha$ -syn were significantly smaller than those without  $\alpha$ -syn and correlated with reduced expression levels of presynaptic proteins.<sup>19</sup> These findings in human patient material resemble synaptic phenotypes we observed as a result of targeted  $\alpha$ -syn accumulation in *Drosophila*; they support recent experimental findings, which indicate that aggregated  $\alpha$ -syn can directly bind and sequester presynaptic proteins.<sup>74</sup> Together with our findings, these data identify presynaptic deficits and the resultant synaptopathy as a conserved pathogenic pathway of accumulating  $\alpha$ -syn.

In addition to alterations in presynaptic proteins, we also detected  $\alpha$ -syn-mediated loss of BRP puncta in *Drosophila*. BRP is required for the structural integrity and function of synaptic AZs,<sup>57</sup> responsible for vesicle docking and exocytosis of neurotransmitters.<sup>54,56</sup> Downregulation or mutational inactivation of BRP has been shown to impair T-bar formation and to reduce evoked synaptic transmission and quantal content.<sup>57</sup> As a result, the neuronal function is affected, resulting in impaired behaviour, which is illustrated by the name *Bruchpilot*, meaning 'crash pilot' in German, referring to the significantly impaired manoeuvring of BRP mutant flies.<sup>57</sup> Given BRPs core function, reduced numbers of

BRP-positive AZs would predict reduced synaptic efficacy and impaired neural transmission in flies that accumulate  $\alpha$ -syn in presynaptic terminals. Indeed, quantification of the SSVEP<sup>37,60</sup> revealed altered synaptic efficacy caused by  $\alpha$ -syn accumulation in *TH>WT- $\alpha$ -syn-EGFP* flies. These observations in *Drosophila* are in line with a recent study in rodents which showed that overexpression of  $\alpha$ -syn caused impairment in the electroretinogram and loss of TH positive amacrine cells in the retina.<sup>75</sup>

Consistent with impaired synaptic transmission, we found that adult flies expressing  $\alpha$ -syn in DA neurons displayed behavioural deficits in spontaneous locomotor activity. Three-day-old *TH>WT- $\alpha$ -syn-EGFP* flies showed a marked reduction in activity and speed, accompanied by a significantly decreased ability to initiate and maintain motor actions, together with longer pauses between each bout of activity. These  $\alpha$ -syn-mediated motor phenotypes became more pronounced in older flies, revealing an age-related progression of the disease that has also been observed in other *Drosophila* models of Parkinson's disease.<sup>32,41,76-79</sup> In addition, flies accumulating  $\alpha$ -syn also displayed akinetic behaviour which was measured by the proboscis extension response that evaluates the response to sugar stimuli, a motor behaviour that is modulated by a single DA cell, the TH-VUM neuron.<sup>69</sup> Remarkably, *TH>WT- $\alpha$ -syn-EGFP* flies showed a significant reduction in their PER response, suggesting that  $\alpha$ -syn accumulation impairs neuronal function.

This conclusion is further supported by the observed  $\alpha$ -syn-mediated alterations in the SSVEP that is regulated by DA-rich lamina neurons in the adult brain of *Drosophila*.<sup>37,60</sup>  $\alpha$ -syn accumulation also caused progressive deficits in negative geotaxis, a startle induced locomotor behaviour that is controlled by dopamine in the fly brain.<sup>32,41,68,79–81</sup> These findings demonstrate that  $\alpha$ -syn-mediated synaptic alterations and impaired neurotransmission cause motor deficits in *Drosophila* affecting voluntary behaviour including action initiation and maintenance, as well as reflex activity. Comparable phenotypes have been observed in rodent models of synucleinopathies and patients with  $\alpha$ -syn pathology (reviewed by Lashuel et al.<sup>92</sup> and Bridi and Hirth<sup>5</sup>). Together these data strongly suggest that presynaptic accumulation of  $\alpha$ -syn causes synaptopathy and progressive behavioural deficits.

Accumulation and aggregation of  $\alpha$ -syn are believed to cause a vicious cycle in DA neurons, triggering further accumulation of  $\alpha$ -syn and neuronal cell death.<sup>5</sup> Our experiments in *Drosophila* demonstrate that accumulating  $\alpha$ -syn causes progressive degeneration of DA neurons in an age-related manner. Interestingly,  $\alpha$ -syn accumulation preferentially affected both PPL1 and PPM3 cluster of DA neurons that regulate motor behaviour and are specifically affected in *Drosophila* models of Parkinson's disease.<sup>76,82–84</sup> These findings resemble what is seen in Parkinson's disease patients where the reduction in nigrostriatal pathway connectivity occurs prior to the degenerative cell death of DA neurons in the substantia nigra pars compacta.<sup>21,26</sup> Of note, the progression of degenerative cell loss in *Drosophila* correlated with the progressive accumulation of  $\alpha$ -syn levels in the ageing animal, illustrating a key characteristic of synucleinopathies, especially Parkinson's disease, in that specific populations of DA neurons are particularly vulnerable to  $\alpha$ -syn burden which directly correlates with disease severity and extent of neurodegeneration.<sup>85</sup>

Alterations in synaptic proteins have been reported in clinical studies of Parkinson's disease, PDD and DLB patients with  $\alpha$ -syn pathology. These studies suggest that axonal and synaptic alterations correlate with cognitive decline and the severity of the disease.<sup>24,25</sup> *In vivo* studies showed that reduced expression of  $\alpha$ -syn was able to ameliorate neurotoxicity and behavioural deficits in conditional transgenic mice.<sup>86</sup> Furthermore, in a transgenic model of DLB/Parkinson's disease, pharmacological targeting of accumulating  $\alpha$ -syn was sufficient to improve behavioural alterations and to ameliorate neurodegeneration.<sup>87</sup> More recent findings indicate that the process of Lewy Body formation, rather than fibril formation of  $\alpha$ -syn, is linked to synaptic dysfunctions that occur before the early onset of neurodegeneration.<sup>88</sup> These findings are in line with our observations in *Drosophila*, which reveal insights into early pathogenesis whereby the presynaptic accumulation of  $\alpha$ -syn affects synaptic proteins and impairs AZ-mediated neuronal function. Consistent with our findings in *Drosophila*, we found that the AZ matrix

protein Liprin- $\alpha$ 4 is downregulated in the prefrontal cortex of DLB patients which display Parkinsonian phenotypes along with dementia.<sup>20,40</sup> Despite  $\alpha$ -syn pathology being the defining feature of DLB, this disorder is often accompanied by other age-related neurodegenerative pathologies such as amyloid plaques and tau tangles<sup>89</sup> that may contribute to the observed phenotypes, which remains to be determined. Nevertheless, our findings are consistent with a pathogenic mechanism where synaptic alterations directly correlate with cognitive decline in Parkinson's disease, DLB and PDD patients.<sup>40</sup>

Taken together, our results presented here indicate  $\alpha$ -syn accumulation in presynaptic terminals affects synaptic proteins and AZ integrity that impair neuronal function. The resultant synaptopathy causes behavioural deficits and progressive age-related neurodegeneration. This succession of phenotypes recapitulates key events of dying-back like neurodegeneration<sup>5,27,90</sup> and provide insights into the pathogenic mechanisms underlying synaptopathy, the likely initiating event in Parkinson's disease and related synucleinopathies.

## Supplementary material

Supplementary material is available at *Brain Communications* online.

## Acknowledgements

We thank R. Faville for help with the DART system; H. Bellen, S. Sweeney and D. Deitcher for antibodies; the Bloomington stocks centre for flies; V. B. Pedrozo for the design and production of the custom-made SING apparatus; and to W. H. Au for helpful discussions and technical assistance.

## Funding

This work was supported by a PhD fellowship from CAPES (Coordenação de Aperfeiçoamento de Pessoal de Nível Superior) Foundation—Ministry of Education of Brazil to J.C.B. (BEX 13162/13–6); funding from Demensfonden, Magnus Bergwalls Stiftelse, Stohnes Stiftelse, Gamla Tjänarinnor to E.B.; funding from La Caixa Foundation (HR17-00595) to P.M.D. and by the UK Medical Research Council (G0701498; MR/L010666/1) and the UK Biotechnology and Biological Sciences Research Council (BB/N001230/1) to F.H.

## Competing interests

B.K. is co-founder of BFCLab LTD. The remaining authors report no competing interests.

## References

- Walker Z, Possin KL, Boeve BF, Aarsland D. Lewy body dementias. *Lancet*. 2015;386(10004):1683–1697.
- Bendor JT, Logan TP, Edwards RH. The function of  $\alpha$ -synuclein. *Neuron*. 2013;79(6):1044–1066.
- Goedert M, Jakes R, Spillantini MG. The synucleinopathies: Twenty years on. *J Parkinsons Dis*. 2017;7(S1):S53–S71.
- Spillantini MG, Schmidt ML, Lee VM-Y, Trojanowski JQ, Jakes R, Goedert M. Alpha-synuclein in Lewy bodies. *Nature*. 1997;388(6645):839–840.
- Bridi JC, Hirth F. Mechanisms of  $\alpha$ -synuclein induced synaptopathy in Parkinson's disease. *Front Neurosci*. 2018;12:80.
- Dauer W, Przedborski S. Parkinson's disease: Mechanisms and models. *Neuron*. 2003;39(6):889–909.
- Cheng HC, Ulane CM, Burke RE. Clinical progression in Parkinson disease and the neurobiology of axons. *Ann Neurol*. 2010;67(6):715–725.
- Lang AE, Lozano AM. Parkinson's disease - First of two parts. *N Engl J Med*. 1998;339(15):1044–1053.
- Lang AE, Lozano AM. Parkinson's disease - Second of two parts. *N Engl J Med*. 1998;339(16):1130–1143.
- Mochizuki H, Choong CJ, Masliah E. A refined concept:  $\alpha$ -Synuclein dysregulation disease. *Neurochem Int*. 2018;119:84–96.
- Ferreira M, Massano J. An updated review of Parkinson's disease genetics and clinicopathological correlations. *Acta Neurol Scand*. 2017;135(3):273–284.
- Klein C, Westenberger A. Genetics of Parkinson's disease. *Cold Spring Harb Perspect Med*. 2012;2(1):a008888.
- Satake W, Nakabayashi Y, Mizuta I, et al. Genome-wide association study identifies common variants at four loci as genetic risk factors for Parkinson's disease. *Nat Genet*. 2009;41(12):1303–1307.
- Simón-Sánchez J, Schulte C, Bras JM, et al. Genome-wide association study reveals genetic risk underlying Parkinson's disease. *Nat Genet*. 2009;41(12):1308–1312.
- Singleton AB, Farrer M, Johnson J, et al. Alpha-synuclein locus triplication causes Parkinson's disease. *Science*. 2003;302(5646):841.
- Kalia LV, Lang AE. Parkinson's disease. *Lancet*. 2015;376(14):1–17.
- Venda LL, Cragg SJ, Buchman VL, Wade-Martins R. Alpha-synuclein and dopamine at the crossroads of Parkinson's disease. *Trends Neurosci*. 2010;33(12):559–568.
- Braak H, Sandmann-Keil D, Gai W, Braak E. Extensive axonal Lewy neurites in Parkinson's disease: A novel pathological feature revealed by alpha-synuclein immunocytochemistry. *Neurosci Lett*. 1999;265(1):67–69.
- Kramer ML, Schulz-Schaeffer WJ. Presynaptic alpha-synuclein aggregates, not Lewy bodies, cause neurodegeneration in dementia with Lewy bodies. *J Neurosci*. 2007;27(6):1405–1410.
- Colom-Cadena M, Pegueroles J, Herrmann AG, et al. Synaptic phosphorylated  $\alpha$ -synuclein in dementia with Lewy bodies. *Brain*. 2017;140(12):3204–3214.
- Burke RE, O'Malley K. Axon degeneration in Parkinson's disease. *Exp Neurol*. 2013;246:72–83.
- Hawkes CH, Del Tredici K, Braak H. A timeline for Parkinson's disease. *Park Relat Disord*. 2010;16(2):79–84.
- Mahlknecht P, Seppi K, Poewe W. The concept of prodromal Parkinson's disease. *J Parkinsons Dis*. 2015;5(4):681–697.
- Berezcki E, Francis PT, Howlett D, et al. Synaptic proteins predict cognitive decline in Alzheimer's disease and Lewy body dementia. *Alzheimer's Dement*. 2016;12(May):1–10.
- Dijkstra AA, Ingrassia A, de Menezes RX, et al. Evidence for immune response, axonal dysfunction and reduced endocytosis in the substantia nigra in early stage Parkinson's disease. *PLoS One*. 2015;10(6):e0128651-
- Caminiti SP, Presotto L, Baroncini D, et al. Axonal damage and loss of connectivity in nigrostriatal and mesolimbic dopamine pathways in early Parkinson's disease. *NeuroImage Clin*. 2017;14:734–740.
- Calo L, Wegrzynowicz M, Santivañez-Perez J, Grazia Spillantini M. Synaptic failure and  $\alpha$ -synuclein. *Mov Disord*. 2016;31(2):169–177.
- Solomon DA, Stepto A, Au WH, et al. A feedback loop between dipeptide-repeat protein, TDP-43 and karyopherin- $\alpha$  mediates C9orf72-related neurodegeneration. *Brain*. 2018;141(10):2908–2924.
- Diaper DC, Adachi Y, Lazarou L, et al. *Drosophila* TDP-43 dysfunction in glia and muscle cells cause cytological and behavioural phenotypes that characterize ALS and FTL. *Hum Mol Genet*. 2013;22(19):3883–3893.
- White KE, Humphrey DM, Hirth F. The dopaminergic system in the aging brain of *Drosophila*. *Front Neurosci*. 2010;4(December):205.
- Friggi-Grelin F, Coulom H, Meller M, Gomez D, Hirsh J, Birman S. Targeted gene expression in *Drosophila* dopaminergic cells using regulatory sequences from tyrosine hydroxylase. *J Neurobiol*. 2003;54(4):618–627.
- Poças GM, Branco-Santos J, Herrera F, Outeiro TF, Domingos PM. Alpha-synuclein modifies mutant huntingtin aggregation and neurotoxicity in *Drosophila*. *Hum Mol Genet*. 2015;24(7):1898–1907.
- Brent JR, Werner KM, McCabe BD. *Drosophila* larval NMJ dissection. *J Vis Exp*. 2009;(24):4–5.
- Ohyama T, Verstreken P, Ly CV, et al. Huntingtin-interacting protein 14, a palmitoyl transferase required for exocytosis and targeting of CSP to synaptic vesicles. *J Cell Biol*. 2007;179(7):1481–1496.
- Rao SS, Stewart BA, Rivlin PK, et al. Two distinct effects on neurotransmission in a temperature-sensitive SNAP-25 mutant. *Embo J*. 2001;20(23):6761–6771.
- Goel P, Li X, Dickman D. Disparate postsynaptic induction mechanisms ultimately converge to drive the retrograde enhancement of presynaptic efficacy. *Cell Rep*. 2017;21(9):2339–2347.
- Petridi S, Middleton CA, Ugbode C, Fellgett A, Covill L, Elliott CJH. In vivo visual screen for dopaminergic Rab  $\leftrightarrow$  LRRK2-G2019S interactions in *Drosophila* discriminates Rab10 from Rab3. *Genes|Genomes|Genetics*. 2020;10(6):1903–1914.
- Faville R, Kottler B, Goodhill GJ, Shaw PJ, van Swinderen B. How deeply does your mutant sleep? Probing arousal to better understand sleep defects in *Drosophila*. *Sci Rep*. 2015;5:8454.
- Shaw RE, Kottler B, Ludlow ZN, et al. In vivo expansion of functionally integrated GABAergic interneurons by targeted increase in neural progenitors. *Embo J*. 2018;37(13):e98163-
- Berezcki E, Branca RM, Francis PT, et al. Synaptic markers of cognitive decline in neurodegenerative diseases: A proteomic approach. *Brain*. 2018;141(2):582–595.
- Feany MB, Bender WW. A *Drosophila* model of Parkinson's disease. *Nature*. 2000;404(6776):394–398.
- Burgoyne RD, Morgan A. Cysteine string protein (CSP) and its role in preventing neurodegeneration. *Semin Cell Dev Biol*. 2015;40:153–159.
- Fernández-Chacón R, Wölfel M, Nishimune H, et al. The synaptic vesicle protein CSP $\alpha$  prevents presynaptic degeneration. *Neuron*. 2004;42(2):237–251.
- Menon KP, Carrillo RA, Zinn K. Development and plasticity of the *Drosophila* larval neuromuscular junction. *Wiley Interdiscip Rev Dev Biol*. 2013;2(5):647–670.
- Zinsmaier KE, Hofbauer A, Heimbeck G, Pflugfelder GO, Buchner S, Buchner E. A cysteine-string protein is expressed in retina and brain of *Drosophila*. *J Neurogenet*. 1990;7(1):15–29.
- Zinsmaier KE, Eberle KK, Buchner E, Walter N, Benzer S. Paralysis and early death in cysteine string protein mutants of *Drosophila*. *Science*. 1994;263(5149):977–980.



47. Burré J, Sharma M, Tsetsenis T, Buchman V, Etherton MR, Südhof TC. Alpha-synuclein promotes SNARE-complex assembly in vivo and in vitro. *Science*. 2010;329(5999):1663–1667.
48. Sharma M, Burré J, Südhof TC. CSP $\alpha$  promotes SNARE-complex assembly by chaperoning SNAP-25 during synaptic activity. *Nat Cell Biol*. 2011;13(1):30–39.
49. Volpicelli-Daley LA, Luk KC, Patel TP, et al. Exogenous  $\alpha$ -synuclein fibrils induce Lewy body pathology leading to synaptic dysfunction and neuron death. *Neuron*. 2011;72(1):57–71.
50. Südhof TC. The synaptic vesicle cycle. *Annu Rev Neurosci*. 2004;27(1):509–547.
51. Greengard P, Valtorta F, Czernik A, Benfenati F. Synaptic vesicle phosphoproteins and regulation of synaptic function. *Science*. 1993;259(5096):780–785.
52. Gitler D, Takagishi Y, Feng J, et al. Different presynaptic roles of synapsins at excitatory and inhibitory synapses. *J Neurosci*. 2004;24(50):11368–11380.
53. Han J, Pluhackova K, Böckmann RA. The multifaceted role of SNARE proteins in membrane fusion. *Front Physiol*. 2017;8(Jan):5.
54. Zhai RG, Bellen HJ. The architecture of the active zone in the presynaptic nerve terminal. *Physiology (Bethesda)*. 2004;19(5):262–270.
55. Südhof TC. The presynaptic active zone. *Neuron*. 2012;75(1):11–25.
56. Wang SSH, Held RG, Wong MY, Liu C, Karakhanyan A, Kaeser PS. Fusion competent synaptic vesicles persist upon active zone disruption and loss of vesicle docking. *Neuron*. 2016;91(4):777–791.
57. Wagh DA, Rasse TM, Asan E, et al. Bruchpilot, a protein with homology to ELKS/CAST, is required for structural integrity and function of synaptic active zones in *Drosophila*. *Neuron*. 2006;49(6):833–844.
58. Kittel RJ, Wichmann C, Rasse TM, et al. Bruchpilot promotes active zone assembly, Ca<sup>2+</sup> channel clustering, and vesicle release. *Science*. 2006;312(5776):1051–1054.
59. Goel P, Dickman D. Distinct homeostatic modulations stabilize reduced postsynaptic receptivity in response to presynaptic DLK signaling. *Nat Commun*. 2018;9(1):1856–
60. Afsari F, Christensen KV, Smith GP, et al. Abnormal visual gain control in a Parkinson's disease model. *Hum Mol Genet*. 2014;23(17):4465–4478.
61. Nippe OM, Wade AR, Elliott CJH, Chawla S. Circadian rhythms in visual responsiveness in the behaviorally arrhythmic *Drosophila* clock mutant Clk Jrk. *J Biol Rhythms*. 2017;32(6):583–592.
62. Heisenberg M. Separation of receptor and lamina potentials in the electroretinogram of normal and mutant *Drosophila*. *J Exp Biol*. 1971;55(1):85–100.
63. Calcagno B, Eyles D, van Alphen B, van Swinderen B. Transient activation of dopaminergic neurons during development modulates visual responsiveness, locomotion and brain activity in a dopamine ontogeny model of schizophrenia. *Transl Psychiatry*. 2013;3(1):e2026–10–e206.
64. Mazzoni P, Shabbott B, Cortés JC. Motor control abnormalities in Parkinson's disease. *Cold Spring Harb Perspect Med*. 2012;2:1–17.
65. Ruan K, Zhu Y, Li C, Brazill JM, Zhai RG. Alternative splicing of *Drosophila* Nmnat functions as a switch to enhance neuroprotection under stress. *Nat Commun*. 2015;6(1):10057.
66. Cording AC, Shialis N, Petridi S, Middleton CA, Wilson LG, Elliott CJH. Targeted kinase inhibition relieves slowness and tremor in a *Drosophila* model of LRRK2 Parkinson's disease. *Npj Park Dis*. 2017;3(1):34.
67. Miquel J, Lundgren PR, Binnard R. Negative geotaxis and mating behavior in control and gamma-irradiated. *Drosoph Information Serv*. 1972;48(March):48–60.
68. Sun J, Xu AQ, Giraud J, et al. Neural control of startle-induced locomotion by the mushroom bodies and associated neurons in *Drosophila*. *Front Syst Neurosci*. 2018;12:6.
69. Marella S, Mann K, Scott K. Dopaminergic modulation of sucrose acceptance behavior in *Drosophila*. *Neuron*. 2012;73(5):941–950.
70. Zürner M, Schoch S. The mouse and human Liprin- $\alpha$  family of scaffolding proteins: Genomic organization, expression profiling and regulation by alternative splicing. *Genomics*. 2009;93(3):243–253.
71. Hornykiewicz O. Biochemical aspects of Parkinson's disease. *Neurology*. 1998;51(2 Suppl 2):S2–S9.
72. Auluck PK, Chan HYE, Trojanowski JQ, Lee VMY, Bonini NM. Chaperone suppression of alpha-synuclein toxicity in a *Drosophila* model for Parkinson's disease. *Science*. 2002;295(5556):865–868.
73. Devine MJ, Gwinn K, Singleton A, Hardy J. Parkinson's disease and  $\alpha$ -synuclein expression. *Mov Disord*. 2011;26(12):2160–2168.
74. Choi M-G, Kim MJ, Kim D-G, Yu R, Jang Y-N, Oh W-J. Sequestration of synaptic proteins by alpha-synuclein aggregates leading to neurotoxicity is inhibited by small peptide. *PLoS One*. 2018;13(4):e0195339.
75. Marrocco E, Indrieri A, Esposito F, et al.  $\alpha$ -Synuclein overexpression in the retina leads to vision impairment and degeneration of dopaminergic amacrine cells. *Sci Rep*. 2020;10(1):9619.
76. Whitworth AJ, Theodore DA, Greene JC, Benes H, Wes PD, Pallanck LJ. Increased glutathione S-transferase activity rescues dopaminergic neuron loss in a *Drosophila* model of Parkinson's disease. *Proc Natl Acad Sci U S A*. 2005;102(22):8024–8029.
77. Humphrey DM, Parsons RB, Ludlow ZN, et al. Alternative oxidase rescues mitochondria-mediated dopaminergic cell loss in *Drosophila*. *Hum Mol Genet*. 2012;21(12):2698–2712.
78. Hindle S, Afsari F, Stark M, et al. Dopaminergic expression of the Parkinsonian gene LRRK2-G2019S leads to non-autonomous visual neurodegeneration, accelerated by increased neural demands for energy. *Hum Mol Genet*. 2013;22(11):2129–2140.
79. Sakai R, Suzuki M, Ueyama M, et al. E46K mutant  $\alpha$ -synuclein is more degradation resistant and exhibits greater toxic effects than wild-type  $\alpha$ -synuclein in *Drosophila* models of Parkinson's disease. *PLoS One*. 2019;14(6):1–16.
80. Riemensperger T, Issa A, Pech U, et al. A single dopamine pathway underlies progressive locomotor deficits in a *Drosophila* model of Parkinson disease. *Cell Rep*. 2013;5(4):952–960.
81. Vaccaro A, Issa A-R, Seugnet L, Birman S, Klarsfeld A. *Drosophila* clock is required in brain pacemaker neurons to prevent premature locomotor aging independently of its circadian function. *PLoS Genet*. 2017;13(1):e1006507.
82. Park J, Lee SB, Lee S, et al. Mitochondrial dysfunction in *Drosophila* PINK1 mutants is complemented by parkin. *Nature*. 2006;441(7097):1157–1161.
83. Trinh K, Moore K, Wes PD, et al. Induction of the phase II detoxification pathway suppresses neuron loss in *Drosophila* models of Parkinson's disease. *J Neurosci*. 2008;28(2):465–472.
84. Cunningham PC, Waldeck K, Ganetzky B, Babcock DT. Neurodegeneration and locomotor dysfunction in *Drosophila* scarlet mutants. *J Cell Sci*. 2018;131(18):jcs216697.
85. Braak H, Del Tredici K, Bratzke H, Hamm-Clement J, Sandmann-Keil D, Rüb U. Staging of the intracerebral inclusion body pathology associated with idiopathic Parkinson's disease (preclinical and clinical stages). *J Neurol*. 2002;249(0):1–5.
86. Lim Y, Kehm VM, Lee EB, et al.  $\alpha$ -Syn suppression reverses synaptic and memory defects in a mouse model of dementia with Lewy bodies. *J Neurosci*. 2011;31(27):10076–10087.
87. Wrasidlo W, Tsigelny IF, Price DL, et al. A de novo compound targeting  $\alpha$ -synuclein improves deficits in models of Parkinson's disease. *Brain*. 2016;139(12):3217–3236.
88. Mahul-Mellier AL, Burtscher J, Maharjan N, et al. The process of Lewy body formation, rather than simply  $\alpha$ -synuclein fibrillization,

- is one of the major drivers of neurodegeneration. Proc Natl Acad Sci U S A. 2020;117(9):4971–4982.
89. Irwin D, Hurtig H. The contribution of Tau, amyloid-beta and alpha-synuclein pathology to dementia in Lewy body disorders. J Alzheimer's Dis Park. 2018;08(04):444.
90. Tagliaferro P, Burke RE. Retrograde axonal degeneration in Parkinson disease. J Parkinsons Dis. 2016;6(1):1–15.
91. West RJH, Lu Y, Marie B, Gao FB, Sweeney ST. Rab8, POSH, and TAK1 regulate synaptic growth in a *Drosophila* model of frontotemporal dementia. J Cell Biol. 2015;208(7):931–947.
92. Lashuel HA, Overk CR, Oueslati A, Masliah E. The many faces of  $\alpha$ -synuclein: From structure and toxicity to therapeutic target. Nat Rev Neurosci. 2013;14(1):38–48.